

AUTOMATED CAE PROCESS FOR THERMO-MECHANICAL LIFING PREDICTION OF A PARAMETERIZED TURBINE BLADE WITH INTERNAL COOLING

B.Nouri¹ and A.Kühhorn¹

¹ Chair of Structural Mechanics and Vehicle Vibrational Technology,
Brandenburg University of Technology Cottbus,
Siemens-Halske-Ring 14, 03046 Cottbus Germany, Nouri@tu-cottbus.de

Key words: CAE Process, Multiphysics Problems, Turbine, Cooling, Finite Element, Finite Volume, Coupled 1D and 3D CFD solver.

Abstract. *For the benefit of higher overall thermodynamic efficiency in gas turbine engines, turbine blades are exposed to an increasingly high heat load, which exceeds the melting temperature of the metal airfoil. A system of internal cooling channels is required to provide sufficient cooling performance. However, the rising commercial pressure on engine manufacturers forces them to develop and produce engines with improved performance and reliability at lower cost in shorter periods than in the past. The turbine blade design techniques nowadays still carried out by optimizations based on steady state simulations. Nevertheless, a complete chain of processes beginning with the geometry and ending with the lifing estimation is difficult, because of the very complex internal cooling channel geometry, the lifing methods of single crystal alloys and the high operating temperature. Local flow phenomena and their associated impact on heat transfer may have significant impact on turbine blade life. In this work, a CAE process is developed which combines the geometry creation and the fluid-thermo-mechanical simulation of a high pressure turbine blade with a conventional cooling system. The sensibility of the S-N lifing curves has put increased importance on the combining of the more accurate 3D CFD and fast 1D CFD.*

1 INTRODUCTION

In the drive for higher cycle efficiencies in gas turbine engines, turbine blades are exposed to an increasingly high heat load. The highly demanding requirements to endure thermal and structural loads, while aiming for high overall efficiency, lead to the design of a system with complex cooling channels. This in turn demands improvements of the internal cooling system and a better understanding of the multidisciplinary prediction of fluid solid interaction. A typical approach to enhance the internal cooling of the turbine blade is by casting angled low blockage ribs on the walls of the cooling channels. In order to be able to simulate different settings of internal cooling channel, it is necessary to build a parametric CAD model of the sophisticated cooling blade, which must be capable of reshaping the internal cooling system with all ribs and film cooling tubes.

The lifing analysis of the turbine airfoil requires a very accurate prediction of the internal metal temperature. One of many lifing criteria of a turbine blade is the Low Cycle Fatigue (LCF) lifing where one cycle is defined by the maximum take-off flight condition. A critical section plane needs to be located with an automated routine, which recognizes in the spherical coordinate system the maximum principal stress gradient with the steepest slope. The gradient will be compared with experimental data similar to the data of Nickel superalloys by Fleury & Ha 2001 [1]. This multiaxial fatigue analysis method is accurate for the prediction of low cycle fatigue, but it requires a high density FEM mesh [1]. The simplified fatigue analysis relationship calibrated by cyclic tests and the stress to number of life cycle curves are well described by Wu 2009 [2].

On the one hand such a demand of accurate temperature prediction can only be fulfilled with a complex 3D-CFD simulation of the whole internal cooling system. On the other hand a 1D-CFD model predicts the internal temperature within seconds. Nonetheless, the 1D-CFD model has to be able to predict local heat transfer effects which are induced by cooling features like ribs or rotational effects. Throughout in this investigation, an approach is presented where 3D-CFD results are used to improve the 1D-CFD predictions [3].

In this paper, the design and development of the CAE process is presented, along with the current status. The paper begin with details on the parametrized CAD model of the high pressure turbine blade Smartblade and its advantages as complete expression based model of a turbine blade with internal cooling. The identification of the 1D CFD flow network is expressed in the next section. The thermal simulation and the coupling to 3D CFD is shown in section 4. Finally it will be shown how the lifing is estimated with the structural simulation. This investigation describes the building of a process chain which will end with an intelligent digital prototype (idq). As stated by [4] "an idq can help to ensure the required quality standard and it saves testing and simulation time". Finally, a Design of Experiment (DOE) example will be shown, where 10 different variations of the blade internal cooling system are assessed with the presented multi-disciplinary process. The design space evaluated turns out to have a range of life expectation from 1060 to approx. 38000 cycles.

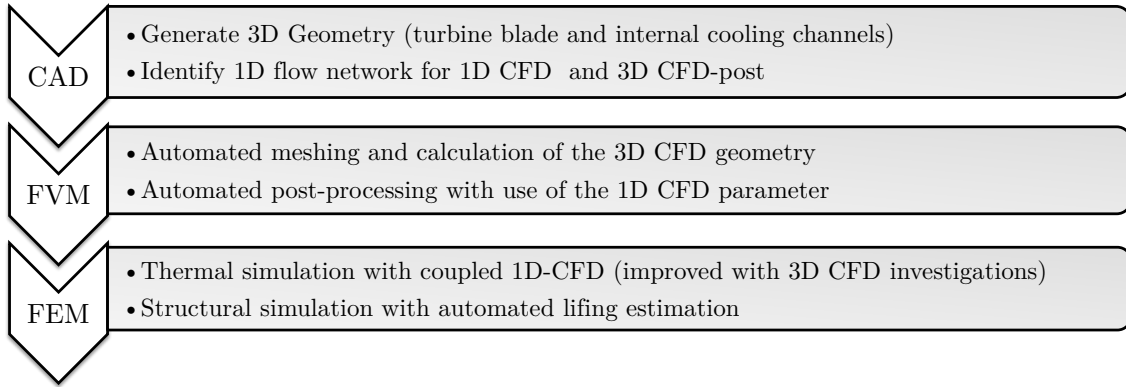


Figure 1: Complete CAE process

2 CAE process

The CAE process chain contains several different aspects of computer aided help for the engineer (figure 1). First a CAD geometry model of the high pressure turbine blade with internal cooling must be built. This is done here with Siemens Unigraphics NX 7.5 and the interface NXOPEN. With this interface it is possible to create a turbine blade with the external aerodynamic boundaries. This model contains complex internal cooling system with five cooling channels and two U-bends. However, information about the path of the internal cooling system is missing. Therefore a tool has been developed which can identify the internal 3D Path.

The goal of this CAE process is a lifing prediction, for which it is essential to predict the local temperature with high accuracy. A possible but costly approach is to simulate external and internal cooling flow with 3D CFD. Nowadays as stated in [8], "3D CFD is used with some confidence in industry and is considered essential as research tool". But the complex geometry with film cooling holes and ribs will force the engineer to mesh the geometry with a high density discretization. Therefore a 1D CFD surrogate model is used, that can take the information of 3D CFD and map an accurate heat transfer prediction on the internal cooling channels.

3 SMARTBLADE AND SMARTCORE

For the purpose to be able to simulate different types of turbine blade geometries an expression based model of the turbine blade with internal cooling system is required. These models are academic versions of a turbine blade with five cooling channels. The external aerodynamic geometry is straight and not optimal, since outer aerodynamic shape is outside the scope of this work.

3.1 Smartblade

The smartblade is an expression driven process which includes CAD scripting in NX with NXOpen. The inputs for this model are the firtree type, the tip type and the external aerodynamic surfaces (pressure side and suction side). It enables to choose between several types of tip and feet shapes which fit with the size of the airfoil.

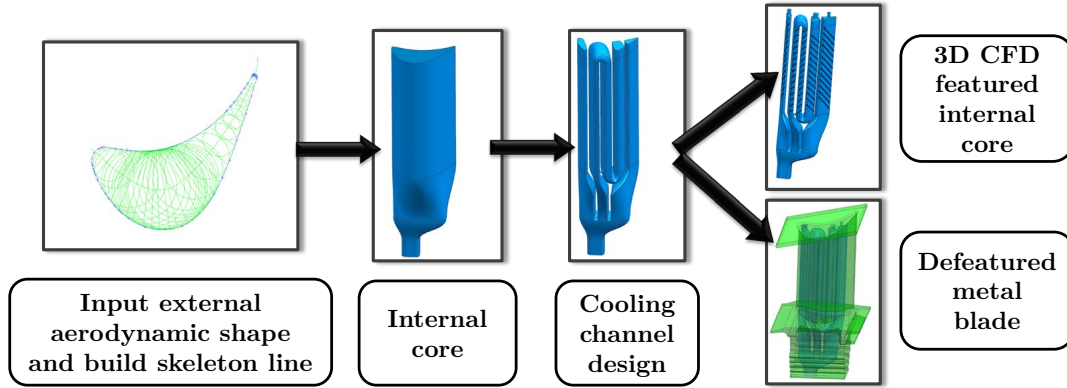


Figure 2: Smartblade + Smartcore: A parametrized scripted UG method to generate a featured CFD geometry (top right air volume is solid) and a defeated metal blade model (bottom right no cooling features)

3.2 Smartcore

This tool is able to generate a complete cooling system with a variable number of internal cooling channels and bends. It also can generate cooling enhancement features, such as ribs and film cooling holes. It delivers a fully blade model defined by expressions with a high flexible (more than 10^{10} possible set of expressions) set of variation. For the here presented numerical investigation, a cooling geometry with five cooling channels is created with low blockage 45° ribs.

4 THERMAL SIMULATION WITH 3D AND 1D CFD

4.1 1D CFD Flow

A surrogate model of the complex internal 3D flow structure is developed. This 1D CFD surrogate model is about 10000 times faster than full 3D CFD but it requires accurate information about the distribution of the internal heat transfer coefficient (figure 3). However it also requires the basic geometric information of the internal system which will vary with every variation of the Smartcore. To obtain this information automatically, a tool in UG NX 7.5 with NXOpen was developed which can identify the internal cooling geometry. It extracts directly from the CAD model the XYZ Data of the middle points (every channel will be analyzed on 30 positions) and the relevant fluid data. For the internal cooling system with low blockage ribs the following parameters are relevant:

- hydraulic diameter D_h
- area A
- perimeter P
- aspect ratio AR (width to height relationship in the internal cooling channel)
- all attached cooling features (ribs or films)

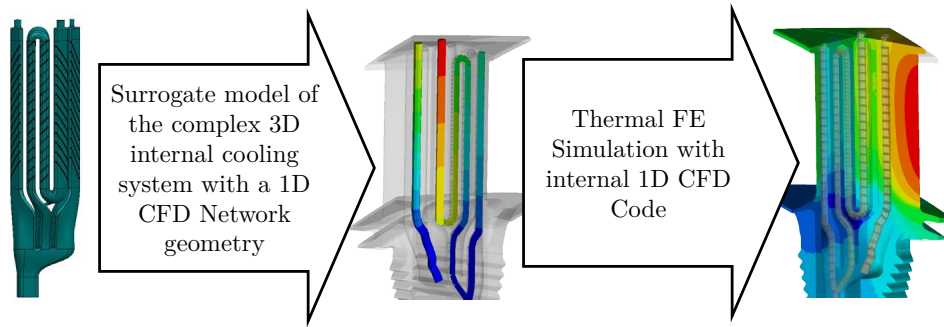


Figure 3: Structural high density mesh

4.2 3D CFD Flow

The pressure based solver used for the analysis is Fluent 14.0. The velocity pressure coupling method used was the coupled method. The material model of air is an ideal gas for density with Sutherland 3 coefficient method for the viscosity. The K-Omega with SST turbulence model was chosen for a compromise of good results and good convergence behaviour. The convergence criteria are constant low residuals (less than $1e-4$) and a maximum difference of 0.01% of the total surface heat flux integral of a section of 5 ribs over 100 iterations.

Table 1: Settings for 3D CFD

<i>CFD</i>	<i>Setting-FLUENT 14.0</i>
cell zone inlet	Mass flow inlet normal to boundary
cell zone outlet	Pressure outlet
solid walls	Wall temperature
solver	Pressure based, implicit 2 nd order discretization
turbulence	K-omega SST

The mesh is a combination of tetrahedral and prismatic elements. The meshing tool which has been used is ICEM from ANSYS. It was created with 16 prismatic layers on all walls. The aim was a non-dimensional wall distance y^+ of 0.3 for ribbed and the smooth surfaces. Each rib is discretized with more than 6 elements in flow direction. The pressure and suction side are in general much finer meshed than the plenum or the surfaces without ribs.

For the post processing a method was developed which can use the 1D CFD parameter

for the 3D CFD heat transfer distribution (figure 4). To acquire the Nusselt number ratio Nu/Nu_0 , several parameters must be extracted as mass flow averaged surface integral in the post processor. The hydraulic diameter is calculated according to:

$$D_h = 4(Area/Perimeter) \quad (1)$$

Several sections on different positions S (channel position from cooling channel beginning to tip) have been made to get the mass averaged local total bulk temperature and the local mean velocity. The Reynolds number for channels is defined by:

$$Re = \frac{\rho U_b(S) D_h}{\mu} \quad (2)$$

where ρ is the local density and U_b is the mean velocity. Polynomial functions are used to approximate the local bulk flow temperature T_b along the S coordinate in the channel. With the local bulk temperature the heat transfer coefficient h is calculated:

$$h = \dot{q}/(T_w - T_b(S)) \quad (3)$$

The local Nusselt number is calculated with the local heat transfer coefficient h and the local thermal conductivity:

$$Nu = h D_h / (k) \quad (4)$$

The fully developed Nusselt number for a turbulent stationary smooth pipe is given by:

$$Nu_0 = 0.023 Re(S)^{0.8} Pr^{0.4} \quad (5)$$

This is the equation from Dittus Boelter/McAdams [1] for smooth pipe where Pr is the local molecular Prandtl number.

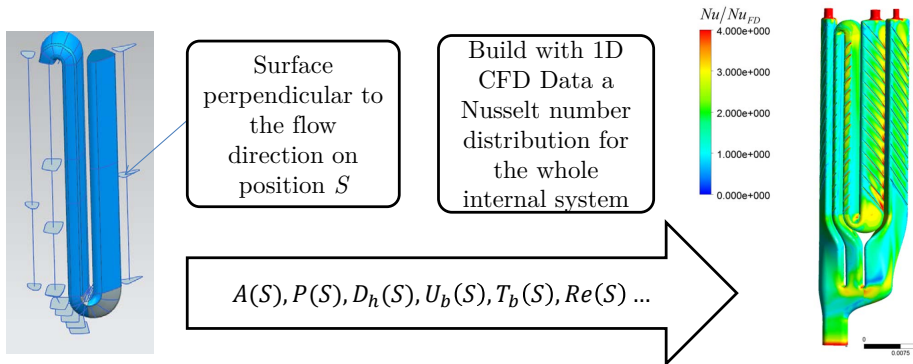


Figure 4: Automated CFD Post processing with use of 1D CFD parameter

4.3 1D and 3D CFD combination

There are three important local Nusselt number surface effects which need to be taken into account for the different cooling flow channels:

- The local enhancement due to the asymmetric geometry of the 45 rib
- The rotational effect
- Impingement at inlet of the film cooling holes

All effects cause high local enhancement of the Nusselt number ratio and therefore should be applied as boundary condition to the thermal simulation of defeatured geometries for lifting simulations and for an accurate temperature prediction. However, since the 1D CFD code in the beginning of this investigation was not able to map local heat transfer solutions a coupled solver has been written, in which the 1D central flow is normalized by the local effects which are mapped to this 1D CFD channel. The cooling channel walls are divided into four different sides and are named according to the position in a turbine blade.

- PS- is the pressure side (Coriolis force in outwards directed rotating cooling channel is directed towards PS)
- SS- is the suction side of the cooling channel
- LE- is the side nearest to the blade leading edge
- TE- is the side nearest to the blade trailing edge

In figure 5 the mapping method is shown for 2 different cooling channels with different height to width ratio (aspect ratio AR), the effect of rotation is a result of the shape of the cooling channel. The function of the Nusselt number ratio distribution is plotted as a function of X. Where X is a normalized distance parameter starting in the corner PS LE and is extending anti clockwise around the cooling channel (figure 5). The maximum of X is 4, each side is 1 long for AR=1. For AR=0.5 the maximum length of X is 3 because two sides are shorter.

The distribution of the Nusselt number ratio disparities between the rotational frame and the stationary frame is significant for small AR. For AR=1 there is a significant difference of the shape of the distribution on the LE and TE side.

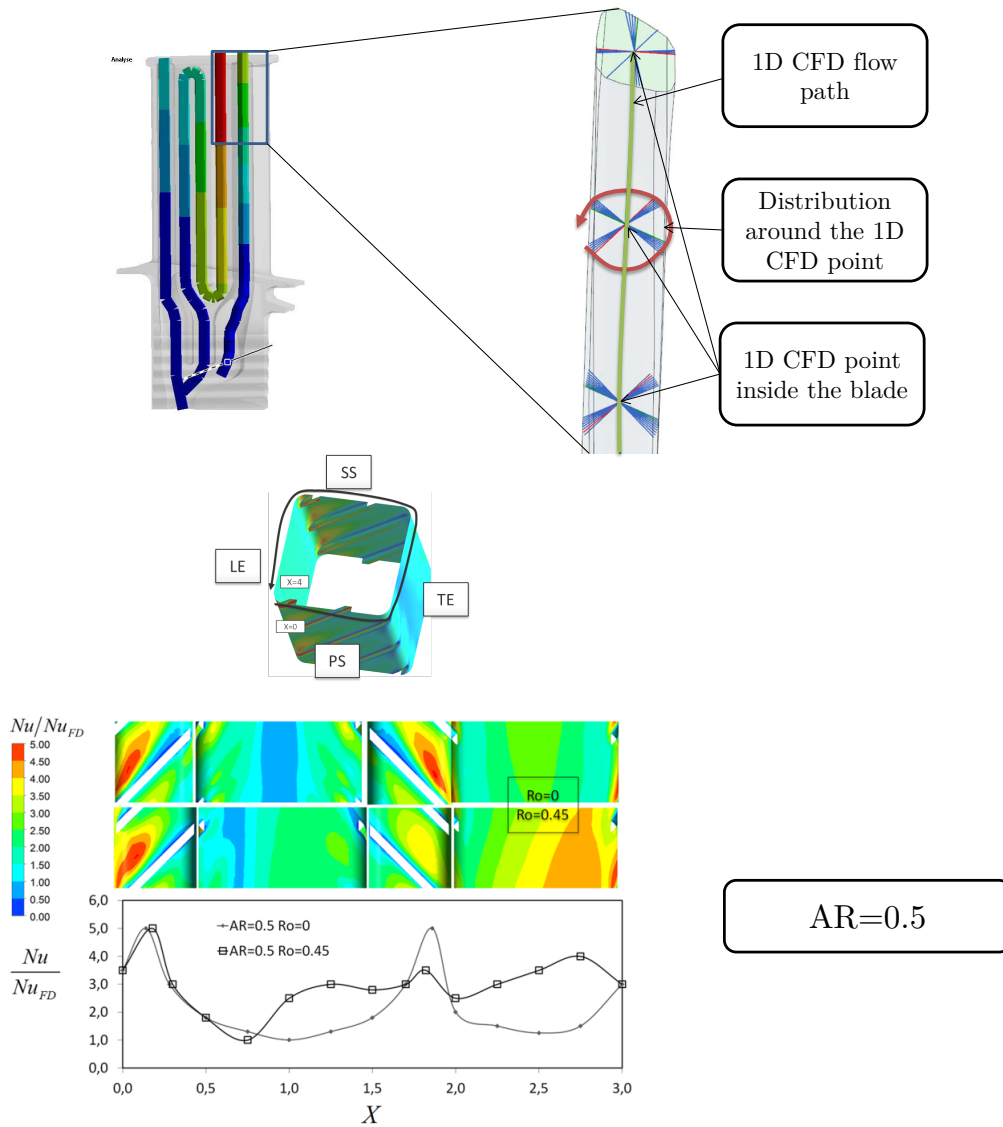


Figure 5: Nusselt number ratio distribution for a 4 wall geometrie with differen aspect ratios and rotation numbers

5 MECHANICAL FE SIMULATION AND LIFING

5.1 FE mechanical

The mesh discretization for the finite element method of the turbine blade is shown in figure 6. This defeatured blade is represented by a solid airfoil attached to a 6% section of the disc platform. Since this investigation is focused on the airfoil section, the platform only serves as the elastic boundary condition. The external temperature and pressure distributions are obtained from a 3D fluid simulation combined with a 2D film cooling efficiency calculation for the hot external surface. The external geometry and boundary condition is set constant for all obtained DOE results. The turbine rotates at 12000 rpm.



Figure 6: Structural high density mesh

The results of the structural simulation showed a high peak of the maximum principal surface stress at the first U-bend where the flow is redirected from cooling channel 2 to cooling channel 3 (figure 7). Although this is not the only region with a significant high local surface stress the following lifing DOE in this paper will focus on this region.

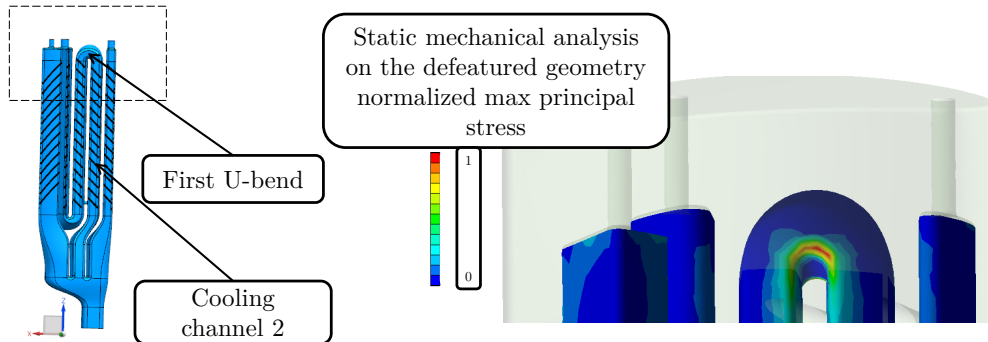


Figure 7: Maximum principal stress at internal surface first U-bend

5.2 Lifing Assessment

A lifing model generally calculates the number of cycles to failure for a certain component to a specific load sequence. The component in this investigation is the turbine blade with internal cooling channel and the load sequence is the maximum take off condition. The basis of this method was the estimation of component life through the construction and use of empirical stress-life (S-N) curves, for the relevant materials. There is high confidence on this method, as stated by [10]: "The methodology has been extensively validated against a database of fatigue results for a typical engine alloy, and has been demonstrated to provide accurate estimates of specimen and component life under extreme combinations of both stress and volume". The LCF data from laboratory test are used to estimate the life of high pressure turbine components with stress concentration features such as connection channels or bends, since it is believed that with the constraint of the surrounding elastic material, the local deformation behavior is leaning more

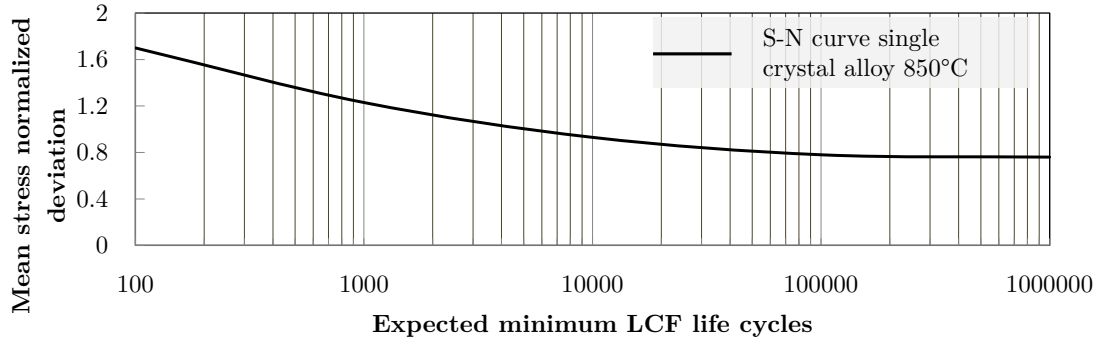


Figure 8: Normalized experimental S-N curve of a nickel based single crystal alloy

towards strain-controlled condition. A good description of the heated specimen and the derivation of the typical S-N curves are in [11]. In figure 8 a normalized mean stress graph of these tests is shown. The sensitivity is enormous for a very low change of the mean stress value the life can increase or decrease by a factor of 10, especially around 10,000 to 100,000 estimated minimum life cycles.

The stress tensor must be reduced twice to get the scalar value. Firstly, a critical plane normal to the spot is selected, within this plane a routine will check and compare all stress gradients and find a direction with the most critical internal stress distribution (figure 9 and 10). This is a multiaxial LCF lifeing methodology similar to the method described by [5]. The combination of \mathbf{d} and \mathbf{n} describes a critical cutplane, it is excepted that the maximum of the cyclic metal degradation is in the direction \mathbf{d} .

$$S_{n,d} = \mathbf{d} \cdot \mathbf{S}_n = \mathbf{d} \cdot (\mathbf{n} \cdot \boldsymbol{\sigma}) \quad (6)$$

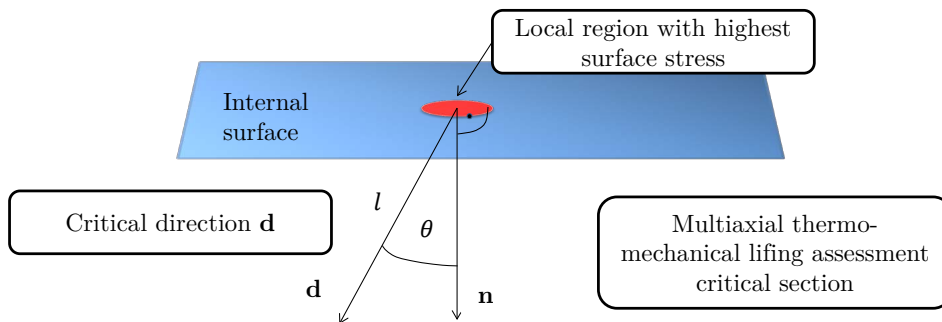


Figure 9: Sketch of critical cut plane and the finding of the steep stress gradient

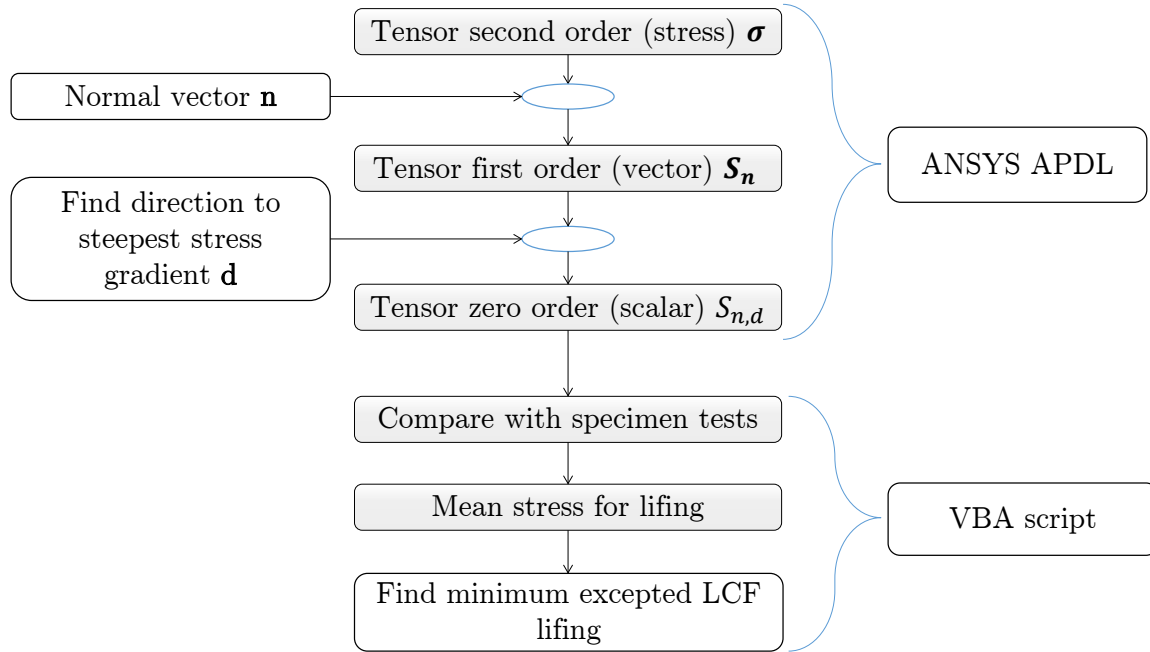


Figure 10: Framework for the lifing methodology

The thermo mechanical multiaxial fatigue lifing method will find the equivalent laboratory specimen with this information a normalized mean stress value is calculated. This normalized stress value is taken to gain the expected minimum LCF lifing (figure 11).

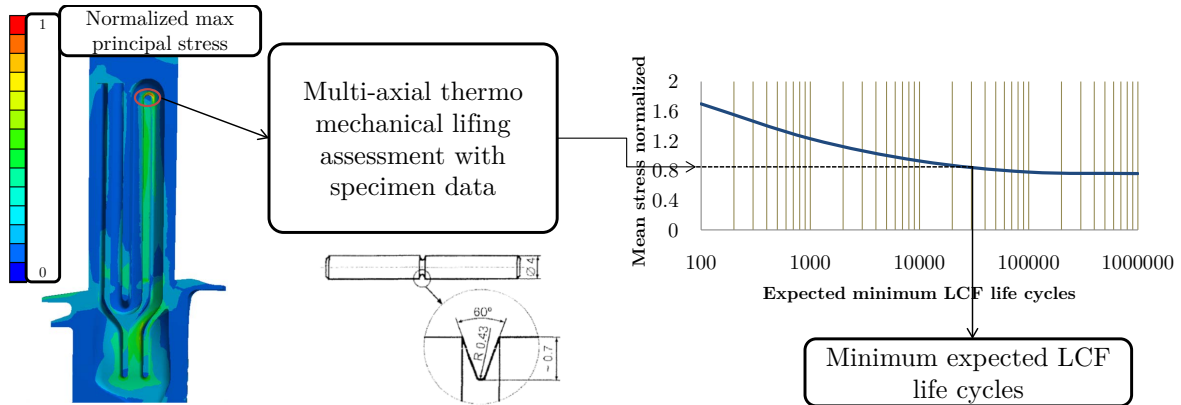


Figure 11: Lifing routine in this CAE process left find highest stress spot, extract from critical plane a steep stress gradient and compare it with laboratory specimen cyclic fatigue test data

6 DOE RESULTS AND DISCUSSION

Firstly, it should be noted that this lifing method is simplified and does not contain HCF, creep, oxidation or other numerical methods which also need to be used to calculate the real life expectation of high pressure turbine blades. To test the earlier discussed CAE process technique with the academic smartblade model, a DOE with 10 different designs

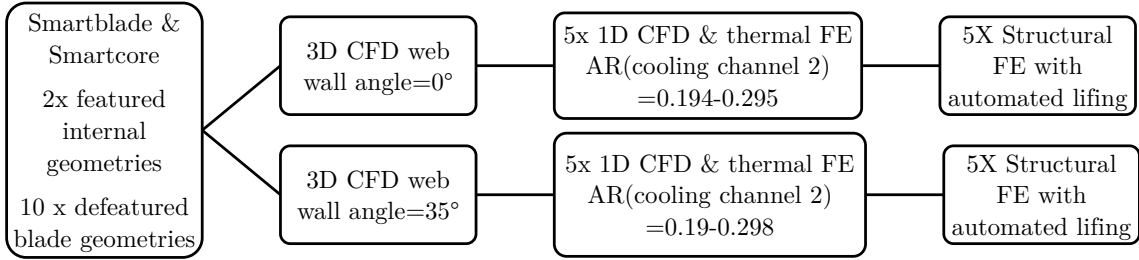


Figure 12: Sketch of the DOE CAE process chain

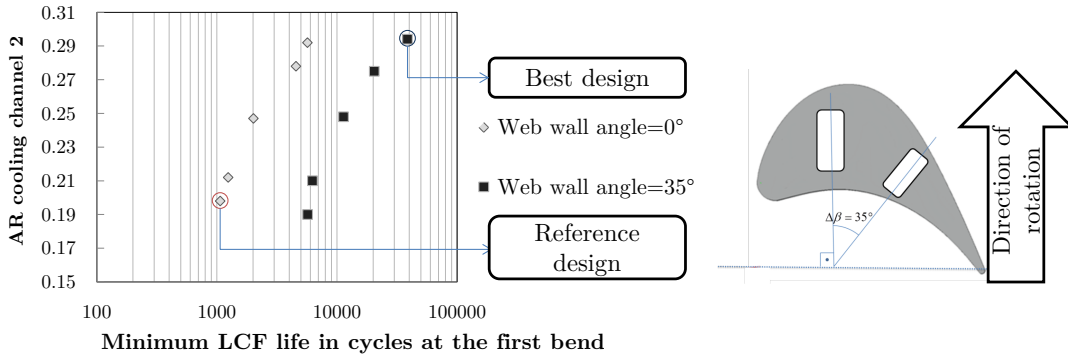


Figure 13: Lifing results of the DOE and description of the web wall angle

was performed and is shown in figure 12. The external heat transfer boundary condition and geometry are kept constant for all computations of the temperature and lifing.

The results of the lifing DOE put into manifest that with a skew $\Delta\beta$ of the web wall angle (the angle of the walls between the cooling channels) the lifing estimation can rise up to nearly 38.000 LCF cycles until the expected failure (figure 13). Figure 14 presents the internal reference cooling geometry of the Smartcore model, together with the geometry that achieves the best expected lifing prediction.

6.1 Discussion

Table 2 brings some data explanation in order to understand the difference of nearly 38.000 expected minimum life cycles between the reference design and the best design, which have the same external boundary condition, the amount of coolant flow, and rotating number.

The heat transfer is in the best design significantly higher, therefore the temperature is lower. Additionally, this lower temperature is combined with a lower maximum principal stress at the spot with the highest surface stress in the first bend. The sensibility of the S-N curve is responsible that a very small variation of the mean stress value can result in a massive variation of the minimum expected LCF lifing (figure 8). As described by J.C.

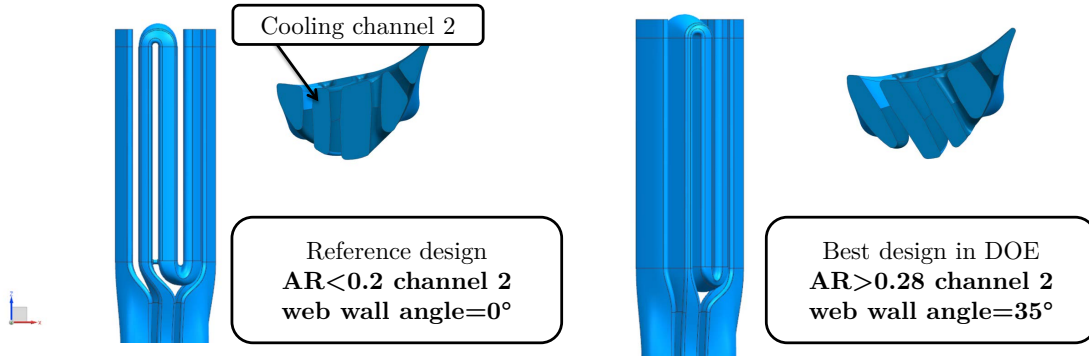


Figure 14: Comparison internal cooling design Reference design left best DOE lifing result right. View from suction side

Han 2013 [7] "It is widely accepted that the life of a turbine blade can be reduced by half if the temperature prediction of the metal blade is off by only 30C." It should be noted that for this particular case not only the maximum temperature and surface peak stress decreased, the parameter which influenced the lifing most is the internal rapid change of the stress in direction d caused by the wider channel 2 and the web wall angle change.

Table 2: Settings for 3D CFD

Data on the spot with highest local principal stress at the suction side of the first bend	Difference between the best (AR=0.29 and $\Delta\beta = 35^\circ$) and reference design (AR=0.192 and $\beta = 0^\circ$)
Temperature	-25.54K
Internal heat transfer coefficient	+20.7%[W/m ² K]
Max principal stress	-14,5%[Pa]
Minimum LCF lifing Factor	36,02

The higher heat transfer can be explained of the skewed web wall angle as shown in [3] a skew of the web wall angle by 35 does distribute the cooling flow more uniform between pressure and suction side of the cooling channel (figure 15). The correction factor for ribbed channels with different aspect ratio is in good comparison with the experimental setup from Azad 2007 [6]. Without the influence of the internal metal stress distribution, which is responsible for a significant lower value of mean stress, and only with consideration of temperature and stress decrease between reference and the best design the lifing factor would only increase to 12 and not to 36.

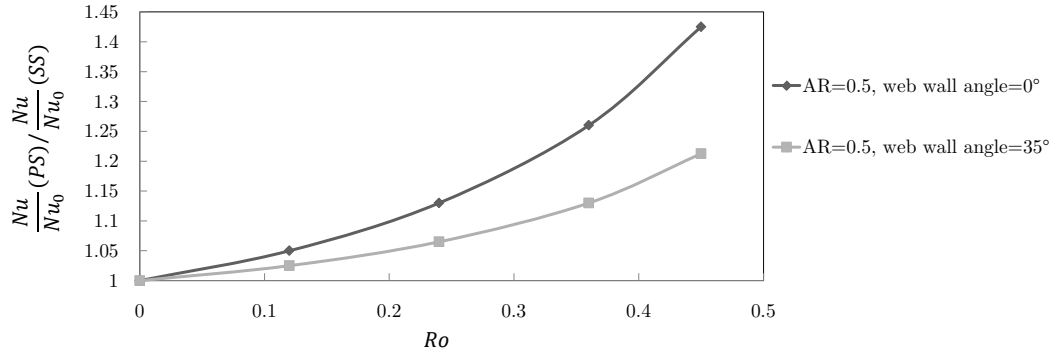


Figure 15: Influence of the web wall angle and the distribution of coolant flow efficiency between pressure side and suction side of the internal cooling channel walls [3]

7 CONCLUSIONS

In order to generate and simulate an intelligent digital prototype of a high pressure turbine blade in an CAE environment it is important to use an innovative design approach and implement accurate physical correlations for a fast solver which than gives the user the ability to optimize the design of a complex internal cooling flow geometry. The combination of 3D CFD and 1D CFD is used to reduce the simulation time by a factor of 10000, however the outcome is a very accurate 3D thermal field. The enhanced 1D CFD model is essential because the 3D Fluid forces have a small impact on surface temperature and heat transfer but a massiv influence on the lifing factor. The automated lifing simulation with LCF can deliver a good start point for the real lifing simulation with HCF lifing and TBC lifing estimation. Generally it can be said that this process could be used with real shaped external blade geometries.

8 OUTLOOK

This CAE process chain does not include a tool for oxidation or HCF lifing. Additional to the multiaxial LCF model, a multiaxial formulated creep model could be implemented, as shown by [9]. Moreover, it opened potential to automate investigations for newer cooling approaches. Unregular V shaped ribs and grooves with a high TPF could be implemented and it would bring the possibility for the first assessment of unconventional cooling geometries like cyclone cooling channels.

9 ACKNOWLEDGMENTS

This work has been carried out in collaboration with Rolls-Royce Deutschland as part of the research project VIT 3 (Virtual Turbomachinery, contract no. 80142272) funded by the State of Brandenburg and Rolls-Royce Deutschland. Rolls-Royce Deutschlands permission to publish this work is greatly acknowledged. Special thanks also to Roland Parchem from Rolls-Royce for his ideas and guidance.

REFERENCES

- [1] Fleury, E. & Ha, J.S.: *Thermomechanical fatigue behaviour of nickel base superalloy IN738LC: Part 2–Lifetime prediction.*, T17, pp. 1087-1092.
- [2] Wu, X.J., Yandt, S. & Zhang, Z. (2009): *A Framework of Integrated Creep-Fatigue Modelling*, Proceedings of the ASME Turbo Expo 2009, GT2009-59087, June 8-12, 2009, Orlando, Florida, USA.
- [3] Nouri, B., Lehmann, K., Kühhorn, A. *Investigations on nusselt number enhancement in ribbed rectangular turbine blade cooling channels of different aspect ratios and rotation numbers* Paper GT2013-94710 , Proceedings of ASME Turbo Expo 2013, June 3-7, San Antonio, Texas, USA
- [4] F. Linares, Z. Zamperin, N. Gramegna, L. Furlan: *iDP approach to quality assessment and improvement of diecasting process*, TCN-CAE 2003, International conference on Cae and Computational Technologies for industry.
- [5] Gaier C., Hofwimmer K., H. Dannbauer H. *Genaue und effiziente Methode zur multiaxialen Betriebsfestigkeitsanalyse* Nafems online magazin , Nr. 4, p.79-89, 2013.
- [6] Azad, G. S., Uddin, M. J., Han, J. C., Moon, H. K., and Glezer, B., 2002, *Heat Transfer in a Two-Pass Rectangular Rotating Channel with 45-Deg Angled Rib Turbulators*, ASME J. Turbomachinery, Vol. 124, pp. 251-259.
- [7] Han, J.C. ; Dutta, S. ; Ekkad, S.: *Gas turbine heat transfer and cooling technology*. 2nd ed. Boca Raton and Fla : CRC Press, 2013. ISBN 9781439855683
- [8] J. W. Chew and N. J. Hills, *Computational fluid dynamics for turbomachinery internal air systems*, (eng),Philos Trans A Math Phys Eng Sci, vol. 365, no. 1859, pp. 2587 2611, 2007.
- [9] Rauer, G., Kühhorn, A., Springmann, M. *Residual Stress Simulation of an Aero Engine Disc during Heat Treatment* Proceedings of the 6th European Congress on Computational Methods in Applied Sciences and Engineering (ECCOMAS 2012), September 10-14, 2012, Vienna, Austria, ISBN: 978-3-9502481-9-7
- [10] Shepherd D.P., and Williams,S.J. *New Lifing Methodology for Engine Fracture Critical Parts* Aging Mechanisms and Control. Symposium Part A - Developments in Computational Aero- and Hydro-Acoustics. Symposium Part B - Monitoring and Management of Gas Turbine Fleets for Extended Life and Reduced Costs 2001
- [11] Lindemann J., Roth-Fagaraseanu D. and Wagner H. *Effect of Shot Peening on Fatigue Performance of Gamma Titanium Aluminides* Conf Proc: ICSP-8 Sept. 16-20, 2002 Garmisch-Partenkirchen, Germany

Table 3: Nomenclature and Abbreviation

PS	Pressure side
TE	Trailing edge side
SS	Suction side
LE	Leading edge side
AR	Channel aspect ratio
D_H	Channel hydraulic diameter $2WH/(W+H)$
\mathbf{d}	Direction to steepest gradient
k	Local thermal conductivity of air
Pr	Prandtl number
\dot{q}	Local surface heat flux
LCF	Low cycle fatigue
HCF	High cycle fatigue
Nu	Nusselt Number
Nu_0	Nusselt number for fully developed turbulent flow in a stationary smooth pipe
Re	Reynolds number
Ro	Rotation number: $\Omega D_H / U_b$
S	Distance from the inlet of the rectangular ribbed duct
T_b	Bulk mean temperature
T_w	Local wall temperature
W	Flow channel width
AR	Aspect ratio width to height W/H
U_b	Bulk flow velocity of the cooling air
X	Length variable on the cooled surface perpendicular to the Z-axis
β	Orientation angle from cooling channel to the rotation axis Web wall angle
ρ	Local air density
σ	Stress Tensor
μ	Local air viscosity